Tsujimoto *et al.* demonstrated reduced contrast effect and phagocytic activity *in vitro* in a rat model prepared by a choline-deficient l-amino acid-defined (CDAA) diet.[10] However, they did not prove it *in vivo* in a rat model that the decreased parenchymal enhancement with Levovist was attributed to phagocytosis by KCs. Sonazoid (GE Healthcare, Oslo) has also been proven to be phagocytosed by KCs.[11,12] We performed CEUS using Sonazoid on a rat NASH model prepared by a methionine choline deficient diet (MCDD)[13] to evaluate the parenchymal enhancement. The phagocytosis of Sonazoid by phagocytic cells was observed *in vivo* in real time by intravital microscopy. To evaluate and prove Sonazoid phagocytosis *in vitro*, isolated and cultured KCs were observed and compared between the MCDD and control groups. Moreover, to evaluate the phagocytic capacity of KCs, the uptake of fluorescein isothiocyanate (FITC)-labeled latex beads was observed and a quantitative analysis was performed using flow cytometry.

METHODS

Animals

THIS STUDY PROTOCOL was approved by the Animal care committee of the Hyogo College of Medicine, and was performed in conformity with their institutional guidelines.

Male Wistar rats (190–200 g; SLC Japan, Tokyo), were housed in the animal facility of the Hyogo College of Medicine and kept at a controlled temperature of 23 ± 1~2°C under 12 h light/12 h dark cycles. Animals for the NASH model were given free access to tap water and MCDD (Oriental Yeast, Tokyo). Animals in the control group had free access to tap water and a normal laboratory diet (MF diet; Oriental Yeast). Animals on the 2nd, 4th and 8th weeks of the diet were used. For observation by intravital microscopy, 25% urethane (Wako Pure Chemical Industries, Osaka) subcutaneous anesthesia was used; and for other observations, isoflurane (Takeda Pharmaceutical, Tokyo) inhalation anesthesia was used.

Histological examination

The liver tissues were fixed in 10% formalin, and then stained with hematoxylin and eosin or Azan. Then, the degree of steatosis, inflammation and fibrosis were assessed from the tissues using the Brunt's histological grading and scoring system.

Preparation of contrast agents and latex beads

The contrast agent Sonazoid and 2.6% FITC-labeled latex beads (Polyscience, Warrington, PA) with diameters of 1 μm and 2 μm, were used. They were diluted with distilled water to 1×10^9 microbubbles/mL and 1×10^9 beads/mL, respectively.

Contrast enhanced ultrasound using Sonazoid

Sonazoid at 0.015 μL (approximately 1.5×10^4 microbubbles)/100g body was injected into the caudal vein after being diluted with distilled water to a total volume of 500 μL.

CEUS was performed by a Toshiba Aplio (Toshiba Medical Systems, Tokyo) with a 7.5 MHz linear transducer. Following conventional B-mode imaging, images were obtained in Advanced Dynamic Flow (ADF) mode with a high mechanical index (MI) of 1.0 to cause destructions of the Sonazoid bubbles. The images were obtained at a focus depth of 3 cm from the body surface at a frame rate of 10 frames/second.

Scanning was performed in various planes of the liver at 20 and 50 min after the Sonazoid injection. This scanning time was based on evidence that the Kupffer phase started at approximately 20 min after the Sonazoid injection when the washout of Sonazoid from the hepatic vein was observed in a healthy volunteer.[14] On the 2nd, 4th, and 8th weeks of the diet, CEUS was performed on four animals from each group to see if any differences in parenchymal enhancement could be detected depending on the duration of the diet. CEUS using ADF was performed at 20 min after the Sonazoid injection to measure the parenchymal intensity within the region of interest (ROI), which was randomly set in the depth within the focus area. The average signal intensity in the liver parenchyma was then calculated after it was converted to sound pressure using the antilog calculation. Scanned images were recorded separately as ADF signals and gray scale signals.

Intravital microscopic observation of phagocytosis by Kupffer cells

Animals in both groups were opened under anesthesia to expose their livers, and were placed in a prone position on a 3 cm diameter transplant platform. A 23 gauge indwelling cannula was inserted into the caudal vein, and 500 μL of 150 μL/100 g Sonazoid diluted with distilled water was administered.

Preparation and phagocytosis of Kupffer cells – *in vitro* study

KCs were isolated from animals in both groups with the previously published procedure: After anesthetizing the animals by isofluran inhalation, the portal vein was cannulated with a 20-gauge needle and the inferior vena cava was opened and a perfusion circuit was created.

Briefly, liver non-parenchymal cells were isolated by the pronase-collagenase method as previously described,[15] and eluted fractions were collected using a Beckman J6-MC centrifuge (Beckman Coulter, Fullerton, CA). The cells were washed, and re-suspended in Roswell Park Memorial Institute (RPMI) 1640 supplemented with 10% fetal bovine serum containing 2-ME (50 μM), L-glutamine (2 mM), penicillin (100 U/mL) and streptomycin (100 μg/mL), plated onto plastic dishes 3.5 cm in diameter, and incubated for 24 h. The plastic adherent cells (1×10^6/mL) were then incubated with 3×10^5 Microbubble/ml Sonazoid for 30 min. After washing the plates with culture medium, the uptake of Sonazoid by the isolated KCs was observed by inverted microscopy (TE300-HM-2; Nikon, Tokyo) in a micro-incubator at 37°C in 5% CO_2. The microscopic images were recorded by image analyzing software (Aquacosmos; Hamamatsu Photonics, Shizuoka). The Sonazoid microbubbles phagocytosed by the KCs were then counted.

Observation of phagocytosis by Kupffer cells – *in vivo* study

Confocal laser scanning microscopy (CLSM)

Latex beads (diameter: 2 μm, concentration: 1×10^8/kg) were administered through the caudal vein of animals from both groups. At 60 min after injection, the animals were sacrificed by anesthesia overdose to prepare frozen sections of the liver. The frozen sections were observed by CLSM (LSM510; Carl Zeiss, Jena).

Flow cytometric quantitative analysis of phagocytic capacity of Kupffer cells

Prior to the experiment, we determined the gating area of KCs fraction using purified KCs according to their forward scatter (FSC) and side scatter (SSC) on a flow cytometer. Once the gated area for KCs was determined, it was used for the rest of the experiments. Aliquots of 1×10^8/kg of FITC-labeled latex beads (diameters: 1 μm and 2 μm) were injected in both groups. At 1 h after injection, KCs isolated by the above-mentioned procedure were cultured for 24 h in an incubator at 37°C in 5% CO_2 to purify the KC fraction and reduce the contaminated cells. Following several washes with phosphate buffered saline (PBS), KCs adhered to the bottom of the dishes were detached with 0.25% Trypsin ethylenediaminetetraacetic acid (EDTA; Invitrogen, Tokyo). They were then centrifuged, and RPMI was added to the sediment to make a total volume of 1 mL in a culture tube. KCs in the tube were then analyzed by flow cytometry. The equipment used was a FACScan (BD Bioscience, San Jose, CA).

Statistics

The statistical significance of the signal intensity change in both groups was evaluated using a repeated measures analysis of variance (ANOVA) test. The Kruskal–Wallis test and Scheffe's *F*-test were performed for a comparison of the phagocytic capacity of isolated and cultured KCs between both groups. All data were analyzed by a statistical software package (SPSS, Chicago, IL).

RESULTS

Changes in liver histology

THE HISTOLOGICAL CHANGES were found as follows: the MCDD-2wk group revealed inflammation and steatosis, but no fibrosis. The MCDD-4wk group showed inflammation, steatosis and slight fibrosis, which was equivalent to grade 2/stage 2 of Blunt's grading/staging system. Inflammation and steatosis were found in the MCDD-8wk group, and their fibrosis was more severe than the one in the MCDD-4wk group, and was corresponding to Blunt's grade 2 /stage 3.

Sonazoid CEUS examination

The signal intensity decreased after Sonazoid injection in the MCDD group as compared to the control group. The quantification of the signal intensity at 20 min after injection is shown in Figure 1. The parenchymal intensity in the control group was −5.0 and −5.5 at 20 and 50 min after Sonazoid injection, respectively, but was −13.0 and −13.3 in the MCDD-4wk group, respectively. In the control group, the intensity decreased slightly to −3.5dB, −4.8dB and −5.5dB on the 2nd, 4th and 8th weeks of administration, respectively. In contrast, in the MCDD group, the intensity decreased according to the duration of the diet administration as to −11.5dB, −13.0dB and −20.5dB on the 2nd, 4th and 8th weeks, respectively; this was a significant difference between the groups ($P < 0.05$) (Figs 1,2).

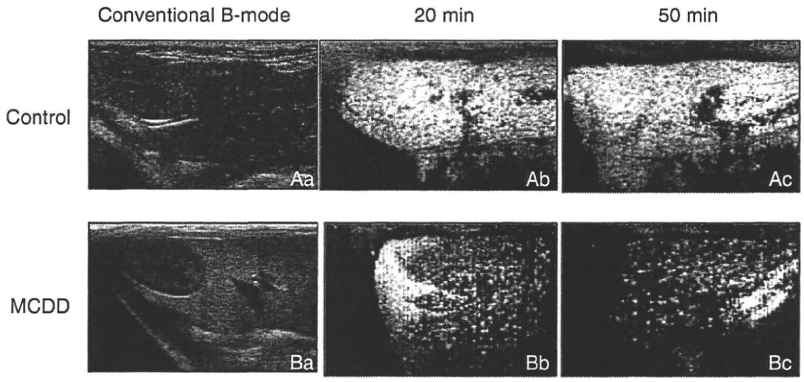

Figure 1 Abdominal US B-mode images (Aa, Ba) and Sonazoid CEUS images (Ab, Ac, Bb, Bc) of control rats (Aa-c) and MCDD-4wk fed rats (Ba-c). The hepato-renal echo contrast was greater in the MCDD rat group as compared with the control group. The livers in the control rats were clearly enhanced until 50 min after injection. In contrast, the enhancement of the liver decreased in the MCDD rats at both 20 and 50 min after injection.

Time course change of Sonazoid phagocytosis observed by intravital microscopy

Five animals from each group were compared. Particles appeared on the sinusoidal wall were observed almost simultaneously at Sonazoid administration, and then the uptake of Sonazoid by phagocytic cells on the sinusoidal wall was recorded using a fixed camera in the view area of the portal vein before Sonazoid injection until 30 min after injection (Fig. 3). The time course was observed by intravital microscopy for 30 min after the Sonazoid injection, and showed that the number of Sonazoid microbubbles phagocytosed by the KCs kept increasing in the control group. However, in the MCDD group, only several Sonazoid microbubbles were phagocytosed by the KCs (Fig. 4).

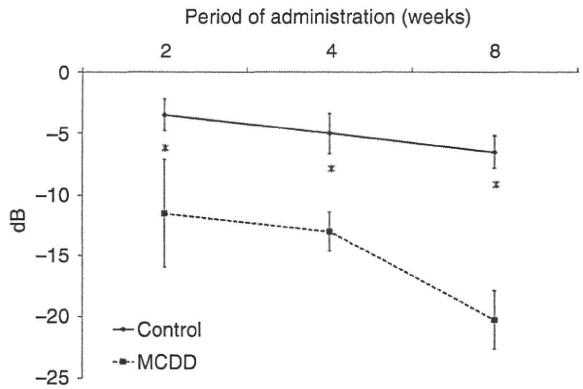

Figure 2 Liver parenchymal intensity (dB) of Sonazoid CEUS on control and MCDD rats at 2 weeks, 4 weeks and 8 weeks of diet administration. The vertical axis is the signal intensity (dB) and the horizontal axis is the duration of diet administration. The parenchymal intensity in the MCDD group showed a decrease as compared with the control group at −11.5dB, −13dB and −20.5dB at the 2nd, 4th, and 8th weeks after administration, respectively ($P < 0.05$).

Phagocytosis of FITC-labeled latex beads by Kupffer cells – *in vivo*

CLSM observations

The number of FITC-labeled latex beads phagocytosed by the KCs and stained as fluorescent green was compared between the two groups. The number of fluorescent-green phagocytosed latex beads in the MCDD group decreased in comparison with the control group, and this suggested decreased phagocytic capacity of the Kupffer cells in the MCDD group (Fig. 5).

Phagocytosis of isolated Kupffer cells – *in vitro*

The inverted microscopic observation of isolated and cultured KCs with Sonazoid is shown in Figure 6. Significant differences were found between the control group and each week of the MCDD groups, and also between the MCDD-2wk and MCDD-8wk groups and between the MCDD-4wk and MCDD-8wk groups ($P < 0.01$) (Fig. 6).

Phagocytosis capability by flow cytometric analysis

Flow cytometric analysis was performed to quantify the phagocytic capacity of isolated and cultured KCs, which were treated with fluorescent latex beads. The phagocytosis rate in the control group was 88%, and many latex beads were ingested. In contrast, the rate was 61% in the MCDD-2wk (B), 37% in the MCDD-4wk (C) and 27% in the MCDD-8wk (D) groups, where the phagocytic capacity had decreased in proportion to the duration

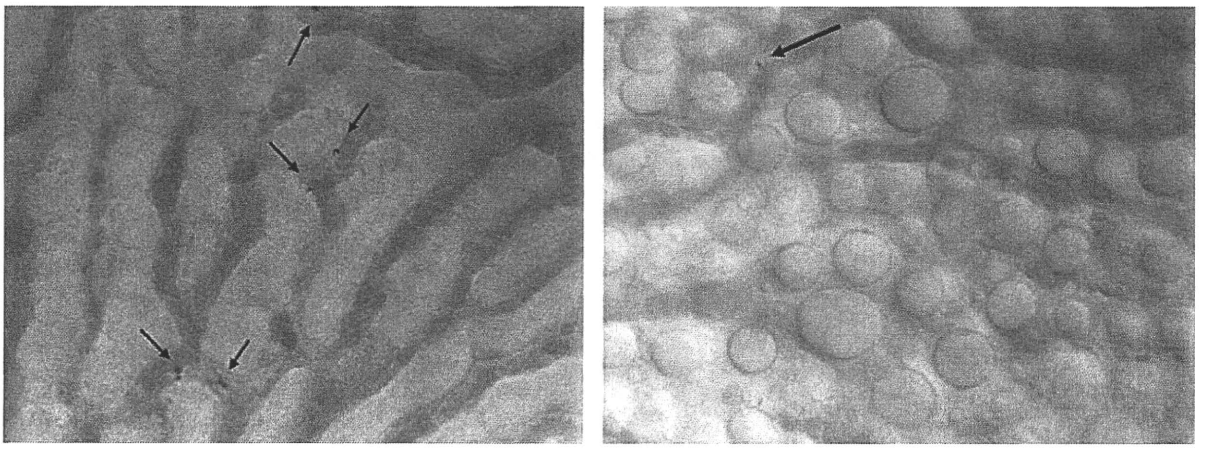

Control rat MCDD rat

Figure 3 Intravital microscopic observation at 30 min after Sonazoid injection. A number of Sonazoid were phagocytosed by phagocytic cells in the control group; whereas a couple of them were phagocytosed in the MCDD-2wk group.

of the MCDD administration. The phagocytosis index (expressed by the number of KCs which phagocytosed beads/the total number of KCs) in the MCDD group was also lower than in the control groups at every duration of the MCDD administration (Fig. 7). This finding revealed that the phagocytic capacity started to decrease at the early stages of the disease, and kept on decreasing week by week.

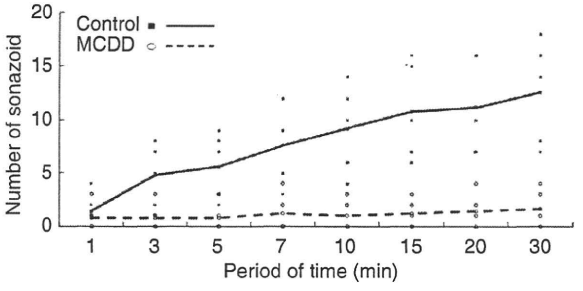

Figure 4 Time-course change in the phagocytosis of Sonazoid. The number of Sonazoid microbubbles phagocytosed by the KCs was plotted at 1, 3, 5, 7, 10, 15, 20 and 30 min after the Sonazoid injection. The control group is shown with a solid line and the MCDD-2wk group is shown with a broken line. Significant difference was seen in the two groups ($P < 0.001$). In the control group, the phagocytosis of Sonazoid increased up to 30 min after Sonazoid injection. In the MCDD-2wk group, only a couple of Sonazoid microbubbles were phagocytosed over a couple min after the injection.

DISCUSSION

NASH HAS BEEN increasing worldwide, and is the most common form of non-alcoholic/non-viral liver disease in the United States and European countries.[16] NAFLD was once considered a benign, reversible condition, and therefore was often left untreated. However, since NASH was introduced by Ludwig, a strong risk of this disease progressing to cirrhosis and hepatocellular carcinoma has been identified.[1-3] In the United States, an estimate shows about 30% of the population has NAFLD, and about 10% of these NAFLD patients has NASH.[17] In countries other than the United States, many people are believed to be developing NASH as their diets become Westernized.[18]

Ultrasonography is used for various organs as a non-invasive diagnostic modality. Ultrasound diagnosis with an intravenous contrast agent is also widely used, and has become indispensable especially in diagnosing the liver diseases.[19,20] The sonographic features of NAFLD including NASH are a high-level echo, a bright liver, vascular blurring, deep attenuation and hepatorenal contrast.[21-24] Abdominal computerized tomography (CT), which provides a more objective assessment, diagnoses NAFLD when the liver to spleen ratio (L/S ratio) is less than 0.9.[25] Thus, the diagnosis of NAFLD could be easily made by these imaging modalities, although distinguishing NASH from NAFLD is considered to be difficult by means of only imaging modalities and blood tests or an invasive liver biopsy is

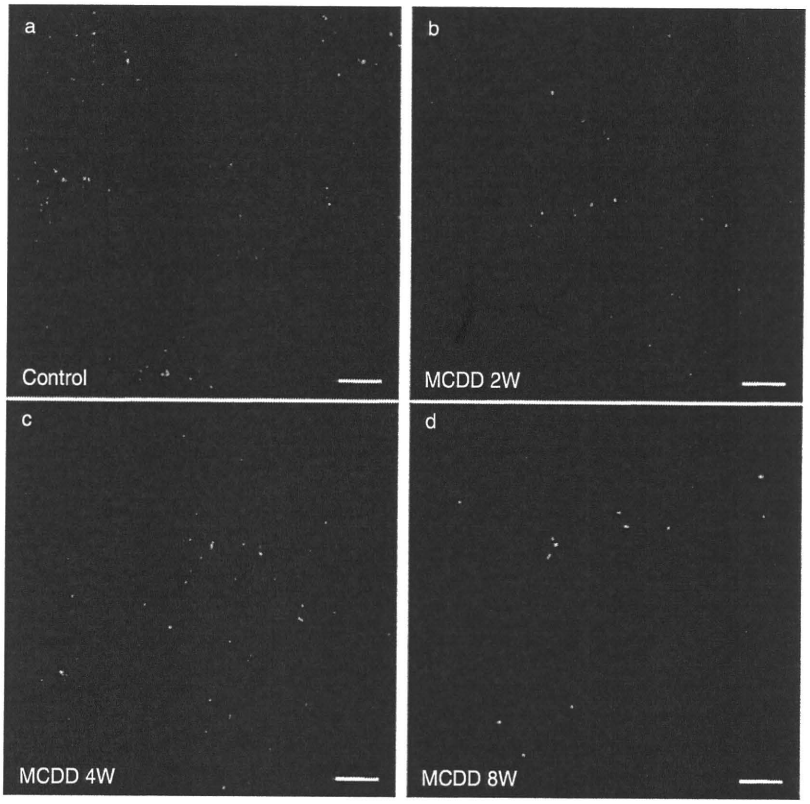

Figure 5 The animals were sacrificed at 60 min after fluorescent latex beads injection and were observed by CLSM. Many latex beads were observed in the control rats (shown in A) as compared with the MCDD rats (in B-D). The fluorescent agent of the latex beads is recognized as green.

required.[4–6] Given the prevalence of NAFLD patients, which has been reported to be as high as 30% of adults who get a medical checkup,[4–6] establishing non-invasive and reliable methods for diagnosing NASH is urgently needed. In the past, we have reported the usefulness of CEUS diagnosis using Levovist to distinguish NASH from NAFLD[9] because it is not realistic to perform liver biopsies for so many NAFLD patients. The diagnosis is made possible by the fact that the liver parenchymal enhancement significantly decreases in NASH patients at 20 min after Levovist injection during the delayed parenchymal phase. One suspected reason for this is the decreased phagocytic capacity of KCs in NASH.[9] Levovist was proven to be phagocytosed by KCs.[11] Furthermore, a study using latex beads on a rat NASH model prepared by a CDAA diet also showed reduced KC phagocytic function, with no changes in the KC numbers, in which the decreased parenchymal contrast effect was possibly attributed to a decrease in the phagocytic capability of KCs, although it did not prove that Levovist itself was phagocytosed by KCs.[10] Moreover, a recent study reported that the engulfment of erythrocytes by KCs was observed by electron microscopy in a rat NASH model induced by a high-fat diet.[26]

Sonazoid is a microbubble with a diameter of 2–4 μm, and contains perfulbutane gas. It has a phospholipid shell which is negatively charged on its surface, and is known to be phagocytosed by liver macrophages, the KCs.[27,28] A report showed that 99% of Sonazoid and 47% of Levovist microbubbles were phagocytosed by isolated and cultured rat KCs;[11] In other words, Sonazoid is expected to be more readily phagocytosed than Levovist. In the present study, the time-course change of KC phagocytosis was investigated by performing CEUS on both MCDD and control rats using Sonazoid by intravital microscopy, and by analyzing isolated and cultured KCs. Sonazoid CEUS performed on a rat NASH model at 20 and 50 min after Sonazoid injection showed a significant decrease in enhancement at 50 min (Fig. 1). Using intravital microscopic observation, the Sonazoid continued to be phagocytosed in the control group, whereas in the MCDD group, the number of phagocytosed Sonazoid

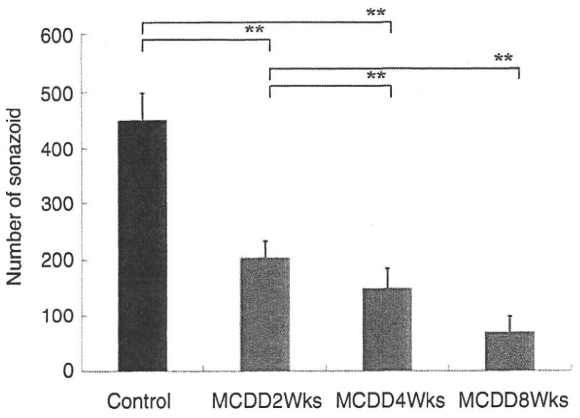

Figure 6 The number of Sonazoid microbubbles phagocytosed by isolated KCs in the control group and the MCDD-2wk, 4wk and 8wk groups were observed by inverted microscopy. After Sonazoid was added, the isolated KCs were cultured before observation. The number of Sonazoid microbubbles phagocytosed by 10 KCs in the control group was 450.5 ± 48.5, whereas 204.1 ± 28.7, 150.9 ± 34.2, and 69.7 ± 29.1 microbubbles were phagocytosed in the MCDD-2wk, 4wk and 8wk groups, respectively (mean ± standard deviation). Significant differences were found between the control group and each week of the MCDD groups, and also between the MCDD-2wk and MCDD-8wk groups and between the MCDD-4wk and MCDD-8wk groups ($P < 0.01$).

microbubbles by phagocytic cells was few after injection. Considering that most of phagocytic cells on sinusoidal wall are KCs, it is reasonable to think contrast agent is phagocytosed by KCs in hepatic sinusoids. Time-course observation also showed the number of phagocytosed microbubbles by phagocytic cells did not increase in the MCDD group (Fig. 4). This finding suggests that the phagocytic capability of KCs may start to decrease during the early stage of NASH, and that could enable the diagnosis of NASH at an early stage of fibrosis. To demonstrate these findings using isolated and cultured KCs, the number of phagocytosed Sonazoid microbubbles decreased in the MCDD rats (Fig. 6). In addition, the number of phagocytosed Sonazoid or latex beads tended to decrease in proportion to the duration of the MCDD administration (Fig. 5). In NASH patients, fibrosis is often detected at a late stage of the disease, because NASH is usually monitored as NAFLD. However, by using Sonazoid CEUS, the diagnosis of NASH could be possible at an early stage, and this represents a groundbreaking development in NASH treatment.

Our study also suggested the clinical usefulness of Sonazoid CEUS in the diagnosis of NASH by demonstrating that: (i) parenchymal enhancement was decreased in the delayed parenchymal phase; and (ii) the phagocytic capacity of Kupffer cells was lowered as the duration of MCDD administration increased. Considering that Sonazoid is specifically phagocytosed by Kupffer cells, the quantification of phagocytic capacity should also be possible.

Some studies have reported the narrowed sinusoids seen in steatosis and steahohepatitis disturb the hepatic microcirculation.[29–31] In particular, the sinusoidal space of a NAFLD animal model was reduced by up to 50 % of the size of healthy control animals.[31] In order to preclude the possibility that the lowered liver parenchymal enhancement was caused by a circulatory disturbance of the contrast agent, latex beads with a diameter of 1 μm, which is smaller than the diameter of Sonazoid (2 μm), were used in the present *in vivo* study, since the width of a normal sinusoid is approximately 5 μm. We performed CEUS with Levovist (4 mL/body) at one minute after Levovist intravenous injection in the early vascular phase to see if decreased parenchymal enhancement was associated with the narrowed sinusoids. Additionally, the parenchymal enhancement of fatty liver patients, NASH patients and healthy volunteers at 1 min after Levovist injection showed a similar intensity in the liver parenchyma in the early vascular phase (Fig. 8). These results demonstrated that the decreased enhancement of liver parenchyma was not due to the narrowed sinusoids or circulatory disturbances.

As shown above, our results suggested decreased Sonazoid-enhanced echogenicity was mainly due to impaired KC phagocytosis, although narrowed sinusoids could be present in MCDD rats due to fatty liver. Sonazoid CEUS could become a useful tool to distinguish NASH patients from many NAFLD patients.

ACKNOWLEDGEMENTS

THIS STUDY WAS supported by a Grant-in-Aid for Scientific Research from the Ministry of Education, Culture, Sports, Science and Technology of Japan, nos. 19500428 and 21300194 and a Grant-in-Aid for Researchers, Hyogo College of Medicine.

We thank all of our colleagues in the Division of Hepatobiliary and Pancreatic Medicine, Ms Sayaka Fujii and Ms Mayumi Yamada, for providing support for our experiments, and the technicians in the Ultrasound Imaging Center.

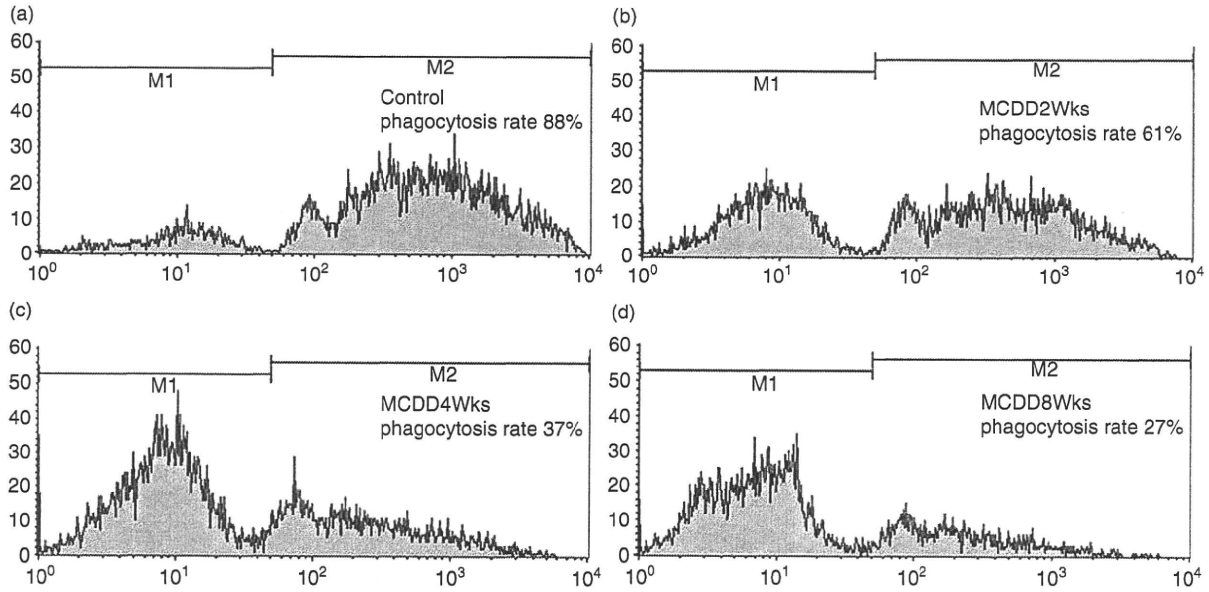

Figure 7 Flow cytometric analysis of isolated and cultured KCs after being treated with fluorescent latex beads. The vertical axis is the KC count and the horizontal axis is the fluorescent intensity. M1 is the number of KCs which did not phagocytose any beads, and M2 is the number of KCs which phagocytosed beads. The phagocytosis rate was calculated by M2/M1 + M2 (the total number of KCs). The phagocytosis rate in the control group was 88% and many latex beads were ingested, whereas the rate was 61 % in the MCDD-2wk (B), 37% in the MCDD-4wk (C) and 27% in the MCDD-8wk (D) groups, where the phagocytic capacity was decreased in proportion to the duration of MCDD administration.

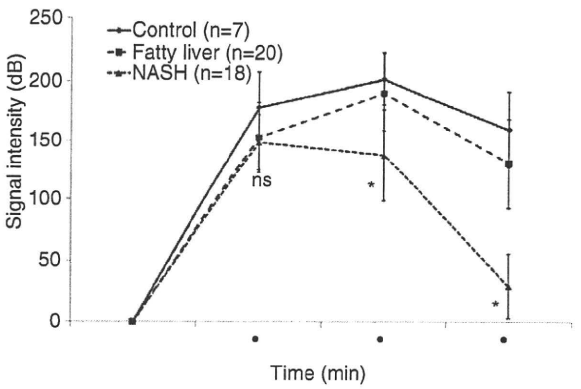

Figure 8 Parenchymal signal intensity in the early vascular phase and the delayed parenchymal phase of Levovist CEUS was evaluated in seven controls (healthy volunteers), 20 fatty liver patients and 18 NASH patients. At 1 min after the Levovist injection, the signal intensity was 178.1 ± 29.3 in the controls, 152.4 ± 30.0 in the fatty liver patients and 148.5 ± 23.6 in the NASH patients (mean ± standard deviation) and no significant differences were observed. However, at 5 and 20 min after injection, there was a significant decrease in the signal intensity in the NASH group.

REFERENCES

1 Ludwig J, Viggiano TR, McGill DB, Oh BJ. Nonalcoholic steatohepatitis: Mayo Clinic experiences with a hitherto unnamed disease. *Mayo Clin Proc* 1980; **55**: 434–8.
2 Bugianesi E, Leone N, Vanni E *et al.* Expanding the natural history of nonalcoholic steatohepatitis: from cryptogenic cirrhosis to hepatocellular carcinoma. *Gastroenterology* 2002; **123**: 134–40.
3 Shimada M, Hashimoto E, Taniai M *et al.* Hepatocellular carcinoma in patients with non-alcoholic steatohepatitis. *J Hepatol* 2002; **37**: 154–60.
4 Saadeh S, Younossi ZM, Remer EM *et al.* The utility of radiological imaging in nonalcoholic fatty liver disease. *Gastroenterology* 2002; **123**: 745–50.
5 Brunt EM, Janney CG, Di Bisceglie AM, Neuschwander-Tetri BA, Bacon BR. Nonalcoholic steatohepatitis: a proposal for grading and staging the histological lesions. *Am J Gastroentero* 1999; **94**: 2467–74.
6 Matteoni CA, Younossi ZM, Gramlich T, Boparai N, Liu YC, McCullough AJ. Nonalcoholic fatty liver disease: a spectrum of clinical and pathological severity. *Gastroenterology* 1999; **116**: 1413–9.
7 Schwenzer NF, Springer F, Schraml C, Stefan N, Machann J, Schick F. Non-invasive assessment and quantification of

liver steatosis by ultrasound, computed tomography and magnetic resonance. *J Hepatol* 2009; **51**: 433–5.
8 Iijima H, Moriyasu F, Miyahara T, Yanagisawa K. Ultrasound contrast agent, Levovist microbubbles are phagocytosed by Kupffer cells-In vitro and in vivo studies. *Hepatol Res* 2006; **35**: 235–7.
9 Iijima H, Moriyasu F, Tsuchiya K, Suzuki S, Yoshida M. Decrease in accumulation of ultrasound contrast microbubbles in non-alcoholic steatohepatitis. *Hepatol Res* 2007; **37**: 722–30.
10 Tsujimoto T, Kawaratani H, Kitazawa T *et al.* Decreased phagocytic activity of Kupffer cells in a rat nonalcoholic steatohepatitis model. *World J Gastroenterol* 2008; **14**: 6036–43.
11 Yanagisawa K, Moriyasu F, Miyahara T, Yuki M, Iijima H. Phagocytosis of ultrasound contrast agent microbubbles by Kupffer cells. *Ultrasound Med Biol* 2007; **33**: 318–25.
12 Watanabe R, Matsumura M, Munemasa T, Fujimaki M, Suematsu M. Mechanism of hepatic parenchyma-specific contrast of microbubble-based contrast agent for ultrasonography: microscopic studies in rat liver. *Invest Radiol* 2007; **42**: 643–51.
13 Weltman MD, Farrell GC, Liddle C. Increased hepatocyte CYP2E1 expression in a rat nutritional model of hepatic steatosis with inflammation. *Gastroenterology* 1996; **111**: 1645–53.
14 Sasaki S, Iijima H, Moriyasu F, Hidehiko W. Definition of contrast enhancement phases of the liver using a perfluoro-based microbubble agent. *Ultrasound Med Biol* 2009; **35**: 1819–27.
15 Tsutsui H, Mizoguchi Y, Morisawa S. Importance of direct hepatocytolysls by liver macrophages in experimental fulminant hepatitls. *Hepatogastroenterology* 1992; **39**: 553–9.
16 Skelly MM, James PD, Ryder SD. Findings on liver biopsy to investigate abnormal liver function tests in the absence of diagnostic serology. *J Hepatol* 2001; **35**: 195–9.
17 Green RM. NASH:hepatic metabolism and not simply the metabolic syndrome. *Hepatology* 2003; **38**: 14–7.
18 Charlton M. Nonalcoholic fatty liver disease: a review of current understanding and future impact. *Clin Gastroenterol Hepatol* 2004; **2**: 1048–58.
19 Harvey CJ, Blomley MJ, Eckersley RJ, Heckemann RA, Butler-Barnes J, Cosgrove DO. Pulse-inversion mode imaging of liver specific microbubbles: improved detection of subcentimetre metastases. *Lancet* 2000; **355**: 807–8.
20 Gaiani S, Celli N, Piscaglia F *et al.* Usefulness of contrast-enhanced perfusional sonography in the assessment of hepatocellular carcinoma hypervascular at spiral computed tomography. *J Hepatol* 2004; **41**: 421–6.
21 Taylor KJ, Carpenter DA, Hill CR, McCready VR. Gray scale ultrasound imaging. The anatomy and pathology of the liver. *Radiology* 1976; **119**: 415–23.
22 Joseph AE, Dewbury KC, McGuire PG. Ultrasound in the detection of chronic liver disease (the 'bright liver'). *Br J Radiol* 1979; **52**: 184–8.
23 Foster KJ, Dewbury KC, Griffith AH, Wright R. The accuracy of ultrasound in the detection of fatty infiltration of the liver. *Br J Radiol* 1980; **53**: 440–2.
24 Yajima Y, Ohta K, Narui T, Abe R, Suzuki H, Ohtsuki M. Ultrasonographical diagnosis of fatty liver: significance of the liver-kidney contrast. *Tohoku J Exp Med* 1983; **139**: 43–50.
25 Ricci C, Longo R, Gioulis E *et al.* Noninvasive in vivo quantitative assessment of fat content in human liver. *J Hepatol* 1997; **27**: 108–13.
26 Otogawa K, Kinoshita K, Fujii H *et al.* Erythrophagocytosis by liver macrophages (Kupffer cells) promotes oxidative stress, inflammation, and fibrosis in a rabbit model of steatohepatitis: implications for the pathogenesis of human nonalcoholic steatohepatitis. *Am J Pathol* 2007; **170**: 967–80.
27 Sontum PC, Ostensen J, Dyrstad K, Hoff L. Acoustic properties of NC100100 and their relation with the microbubble size distribution. *Invest Radiol* 1999; **34**: 268–75.
28 Sontum PC. Physicochemical characteristics of Sonazoid, a new contrast agent for ultrasound imaging. *Ultrasound Med Biol* 2008; **34**: 824–33.
29 Ijaz S, Yang W, Winslet MC, Seifalian AM. Impairment of hepatic microcirculation in fatty liver. *Microcirculation* 2003; **10**: 447–56.
30 McCuskey RS, Ito Y, Robertson GR, McCuskey MK, Perry M, Farrell GC. Hepatic microvascular dysfunction during evolution of dietary steatohepatitis in mice. *Hepatology* 2004; **40**: 386–93.
31 Farrell GC, Teoh NC, McCuskey RS. Hepatic microcirculation in fatty liver disease. *Anat Rec (Hoboken)* 2008; **291**: 684–92.

Original Paper

Influence of Risk Factors for Metabolic Syndrome and Non-Alcoholic Fatty Liver Disease on the Progression and Prognosis of Hepatocellular Carcinoma

Susumu Takamatsu MD, PhD[1], Norio Noguchi MD, PhD[1], Atsushi Kudoh MD, PhD[1]
Noriaki Nakamura MD, PhD[1], Tohru Kawamura MD, PhD[1], Kenichi Teramoto MD, PhD[1]
Tohru Igari MD, PhD[2], and Shigeki Arii MD, PhD[1]

[1]Department of Hepato-biliary-pancreatic Surgery, Tokyo Medical and Dental University Graduate School of Medicine, and [2]Division of Pathology, Tokyo Medical and Dental University Hospital Faculty of Medicine, Tokyo, Japan

Corresponding Author: Susumu Takamatsu, MD, PhD, Department of Hepato-biliary-pancreatic Surgery Tokyo Medical and Dental University, Graduate School of Medicine, 1-5-45 Yushima, Bunkyo-ku, Tokyo 113-8519, Japan

Tel: +81 3 5803 5255, Fax: +81 3 3817 4126, E-mail: s.takamatsu@mac.com

ABSTRACT

Background/Aims: We investigated a relationship between the risk factors for metabolic syndrome, such as obesity, diabetes mellitus, hypertension, and hyperlipidemia, and the pathogenesis and outcome of hepatocellular carcinoma (HCC).

Methodology: One hundred twenty four patients who underwent curative resections for HCC were classified into 3 groups: those patients who were positive for hepatitis B surface antigen (group B), those positive for antibody to hepatitis C virus (group C), and those negative for both of them (non-B non-C) (group NBNC). The preoperative laboratory data, risk factors for metabolic syndrome, history of alcohol abuse, and outcome after surgery were investigated. The presence of non-alcoholic steatohepatitis (NASH) was also evaluated.

Results: The incidence of diabetes mellitus, hyperlipidemia, and alcohol abuse, and the serum level of triglyceride were significantly higher in group NBNC than in groups B or C. The risk factors for metabolic syndrome tended to lower the survival rates in group B and C, but not in group NBNC. Three of the 37 non-B non-C patients were associated with NASH.

Conclusions: It is suggested that the pathogenesis of non-B non-C HCC may be more closely associated with the risk factors for metabolic syndrome than that of hepatitis virus related HCC.

KEY WORDS: Hepatocellular carcinoma; Non-B non-C; Metabolic syndrome; Nonalcoholic steatohepatitis

ABBREVIATIONS: Hepatocellular Carcinoma (HCC); Hepatitis B Virus (HBV); Hepatitis C Virus (HCV); Hepatitis B Surface Antigen (HBsAg); Antibody Against HCV (HCVAb); Metabolic Syndrome (MS) Nonalcoholic Fatty-liver Disease (NAFLD); Nonalcoholic Steatohepatitis (NASH); Anibody Against Hepatitis B Surface Antigen (HBsAb); Antibody against Hepatitis B Core Antigen (HBcAb); Platelet Count (PLT); Asparate Aminotransferase (AST); Alanine Aminotransferase (ALT); Total *Cholesterol (TC); Triglyceride (TG);* Body Mass Index (BMI)

INTRODUCTION

Hepatocellular carcinoma (HCC) is one of the most common cancers, and its incidence has increased worldwide (1). Epidemiological studies and recent molecular biological investigations have revealed that hepatitis B virus (HBV) and hepatitis C virus (HCV) infection are major causes of HCC, and hence numerous basic and clinical studies have been conducted from the view point of hepatitis virus infection (1-6). On the other hand, little attention has been paid to HCC in patients without both hepatitis B surface antigen (HBsAg) and antibody against HCV (HCVAb), possibly because of the small population of these HCC patients (7-12). However, the number of HCC patients without apparent hepatitis virus infection has been increasing, and the so-called non-B non-C HCC has been the subject of investigation in recent years (10,11).

Recently, other factors such as obesity and type 2 diabetes mellitus, which were regarded as risk factors of metabolic syndrome (MS) (13), have been implicated in steatosis and fibrosis of the liver, and HCC (14-18). In addition, although the natural histories of non-alcoholic fatty-liver disease (NAFLD) or nonalcoholic steatohepatitis (NASH) have remained controversial, they have been considered to be one of the possible causes of cryptogenic cirrhosis of the liver and HCC (19-25). However, the relationship between HCC and NASH, as well as the incidence of HCC developing in the liver in response to NASH, has not been well understood. Moreover, the relationship between risk factors for MS, such as hyperlipidemia and hypertension, and HCC still remain unclear.

Based on this point of view, the present study investigated the participation of risk factors for MS in the pathogenesis and progression of HCC, and the outcome after surgical treatment. Evidence will be presented indicating that non-B non-C HCC is more closely related to those diseases with risk factors for MS than HCC associated hepatitis virus infection.

Hepato-Gastroenterology 2008; 55:609-614

METHODOLOGY

A total of 124 patients who underwent curative resections for HCC from April 2000 to March 2005 were enrolled in this study, and their medical records were reviewed retrospectively.

Twenty-six of the 124 patients had already undergone prior treatments including surgery, transcatheter arterial (chemo) embolization, and/or ablation therapy for HCC before being referred to our department.

The patients were divided into 3 groups: groups B, C, and NBNC. Those patients who were positive for HBsAg but negative for HCVAb were classified into the group B, and those who were negative for HBsAg but positive for HCVAb were classified as group C. The NBNC group was composed of the non-B non-C patients. In the non-B non-C patients, the antibody against hepatitis B surface antigen (HBsAb) and the antibody against hepatitis B core antigen (HBcAb) were also measured.

We examined the platelet count (PLT) and serum levels of asparate aminotransferase (AST), alanine aminotransferase (ALT), total cholesterol (TC), and triglyceride (TG) preoperatively. In addition, we investigated the body mass index (BMI), any history of alcohol abuse and risk factors for MS, which consisted of diabetes mellitus, hypertension, and hyperlipidemia (fasting plasma level of TC≥220mg/dL and/or TG≥150mg/dL), in each patient. All of the patients with diabetes mellitus and/or hypertension had already been diagnosed and treated before consulting us. Being overweight was defined as a BMI of 25kg/m^2 or more. A daily ethanol intake of 86g or more for 10 years was regarded as alcohol abuse.

The liver histology as well as the presence of NAFLD and NASH was evaluated in the resected specimens microscopically, especially in those patients without a history of alcohol consumption (daily alcohol intake within 20g) in the NBNC group. If there was moderate to severe macrovesicular steatosis, hepatocellular ballooning, lobular inflammation with necrosis of the hepatocytes and perisinusoidal fibrosis, we considered that NASH was present. The stage of the HCC was defined according to the Japanese general rules of primary liver cancer (26).

After surgical treatment, all of the patients were followed as out patients, and none of the patients underwent adjuvant therapies. Tumor markers such as alpha-fetoprotein and protein induced by vitamin K antagonist-II were measured every month, and ultrasonography, enhanced computed tomography, and/or magnetic resonance imaging were performed every 3 months. If an intrahepatic recurrence was suspected, computed tomography with angiography was performed to confirm.

We calculated the cumulative overall and disease free survival rates in each group, particularly for those patients with and without risk factors for MS.

The data are expressed as means ± standard deviation. Statistical analyses were performed by a one-way analysis of variance for parametric data, and by a Kruskal-Wallis test for categorical data among the three groups. If there was a significant difference on the Kruskal-Wallis test, a further analysis was performed by the Mann-Whitney test with Bonferroni's correction. Both the cumulative overall survival and disease free survival rates were calculated using the Kaplan-Meier method, and comparisons were made by using the log-rank test. A p-value of less than 0.05 was considered statistically significant.

TABLE 1 The Backgrounds of the 124 Patients

	B	C	NBNC	p
N	19	68	37	
Age	55.9±11.3	67.8±6.6	67.7±8.4	<0.0001[a]
Gender (Male/Female)	15 / 4	49 / 19	30 / 7	
Child-Pugh				N.S.
A	18	58	35	
B	1	10	1	
C	0	0	1	
Stage*				N S.
I	1	13	2	
II	5	16	12	
III	7	27	17	
IVA	6	12	6	
Liver histology				0.03[b]
Normal liver	2	0	7	
Chronic hepatitis	8	31	17	
Liver cirrhosis	9	37	13	
Surgical procedure*				N.S.
Hr0	4	31	12	
HrS	8	14	8	
Hr1	2	12	9	
Hr2	5	10	8	
Hr3	0	1	0	
History of previous treatment	3	18	5	

* Stage and surgical procedure were defined according to the general rules for the clinical and pathological study of primary liver cancer, 4th edition. Hr 0: partial resection; Hr S: subsegmentectomy; Hr1: segmentectomy; Hr2: liver resection of 2 segments; Hr3: liver resection of 3 segments. N.S.: Not significant; [a]: B *vs.* NBNC and C; [b]: NBNC *vs.* C

TABLE 2 Preoperative Laboratory Data

	B	C	NBNC	p
AST (IU/L)	58.4±58.0	67.9±37.6	36.7±18.5	<0.001[a]
ALT (IU/L)	47.8±25.3	65.5±46.4	34.1±19.5	<0.001[b]
PLT (×104/mm^3)	15.5±5.5	13.7±7.7	19.6±12.2	<0.01[b]
Total Cholesterol (mg/dL)	174.0±46.3	152.1±35.9	180.1±39.1	<0.01[c]
Triglyceride (mg/dL)	76.0 ± 33.3	95.4 ± 43.9	138.3 ± 81.6	<0.001[a]

[a]: NBNC *vs.* B and C; [b]: NBNC *vs.* C; [c]: NBNC and B *vs.* C

TABLE 3 Associated Conditions

		B	C	NBNC	p
N		19	68	37	
Body Mass Index (kg/m^2)		22.0±3.1	22.8±3.2	24.1±4.1	N.S.
BMI ≥ 25	+/-	4 / 15	12 / 56	11 / 26	N.S.
Diabetes mellitus	+/-	1 / 18	15 / 53	17 / 20	<0 .01[a]
Hypertension	+/-	3 / 16	32 / 36	19 / 18	0.03[b]
Hyperlipidemia	+/-	3 / 16	11 / 57	14 / 23	0.03[c]
Alcohol abuse	+/-	6 / 13	13 / 55	16 / 21	0.03[c]

BMI: Body mass index; N.S.: Not significant; a: NBNC *vs.* B and C; [b]: B *vs.* NBNC and C; [c]: NBNC *vs.* C

RESULTS

Of the 124 patients, there were 94 men and 30 women, and the mean age was 65.9±9.0 years (range 30-82 years). The median postoperative follow-up period was 18.5 months (range 1-58 months).

The number of patients in groups B, C, and NBNC were 19 (15.3%), 68 (54.8%), and 37 (29.8%), respectively. In the NBNC patients, 17 (45.9%) of patients were positive for HBcAb and 16 patients were negative for HBcAb. Four patients were not examined for their HBsAb and/or HBcAb status. The background of these patients is summarized in Table 1. The mean age was significantly younger in group B than in groups C or NBNC ($p<0.0001$). The preoperative Child-Pugh scores were not significantly different among the 3 groups, but there was significant difference in liver histology ($p=0.03$); the incidence of chronic hepatitis and liver cirrhosis was significantly higher in group C than in groups B or NBNC. Both the stage of the HCC and the surgical procedure performed were decided based on the Japanese rules for HCC (26), and were not significantly different among the 3 groups.

Table 2 shows the preoperative laboratory data. Serum level of ALT was lower and the PLT was significantly higher in the NBNC group than in group C. The serum TG level was significantly higher in the NBNC group than in groups B or C.

The BMI and number of overweight patients were not significantly different among the three groups, as shown in Table 3. The frequency of diabetes mellitus was significantly higher in the NBNC group than in either group B or C. The incidences of both hyperlipidemia and alcohol abuse were significantly higher in the NBNC group as compared with group C.

Moreover, we made the same comparisons using those patients without alcohol abuse to exclude the influence of alcohol intake (Table 4). Consequently, we found that the laboratory data were not affected by alcohol abuse, whereas ratios of having associated conditions, such as diabetes mellitus, hyperlipidemia, and hypertension, became statistically insignificant among the 3 groups.

The cumulative overall survival rates at 1 and 3 years in groups B, C, and NBNC were 88.1% / 66.1%, 77.8% / 58.9%, and 85.5% / 69.8%, respectively (Figure 1). There were no significant differences among the three groups ($p=0.46$). The disease free survival rates at 1 and 3 years in groups B, C, and NBNC were 48.5% / 29.1%, 56.5% / 22.5%, and 73.8% / 27.6%, respectively (Figure 2). Although the NBNC group tended to be higher, the differences in the disease free survival rates among these three groups were not significant ($p=0.12$). In addition, to estimate the influence of risk factors for MS on survival after surgery, we compared the cumulative overall (Figure 3) and disease free (Figure 4) survival rates between those patients with *vs.* those without risk factors for MS in each group. In groups B and C, there was a trend that the survival rate was better in those patients without risk factors for MS. On the other hand, the survival rate was slightly better with risk factors for MS in the NBNC group. However, there were no significant differences between the groups. In groups B and C, the disease free survival rate was almost same with *vs.* without the risk factors for MS, and they were not significantly different in each group. In the NBNC group, the disease free survival seemed to be better in those patients with the risk factors for MS, but again there was no statistically significant difference ($p=0.24$).

Moreover, in the NBNC group, the overall ($p=0.50$) and disease free ($p=0.15$) survival rates were not significantly different between the two subgroups

TABLE 4 Laboratory Data, Liver Histology, and Associated Conditions in Patients without Alcohol Abuse

		B	C	NBNC	p
N		13	55	21	
AST (IU/L)		69.0±67.3	68.6±38.0	38.3±19.4	0.01[a]
ALT (IU/L)		52.6±27.1	63.9±45.3	39.0±21.5	< 0.05[b]
PLT ($\times 10^4$/mm^3)		16.3±6.5	13.1±7.9	21.6±14.0	< 0.01[b]
Total Cholesterol (mg/dL)		173.1±54.2	151.7±30.0	184.6±38.5	< 0.01[b]
Triglyceride (mg/dL)		76.4±34.6	95.3±39.4	124.1±69.7	< 0.05[a]
Liver histology					0.001[b]
Normal liver	1	0	5		
Chronic hepatitis	5	20	11		
Liver cirrhosis	7	35	5		
Diabetes mellitus	+/-	0 / 13	11 / 44	7 / 14	N.S.
Hypertension	+/-	3 / 10	27 / 28	9 / 12	N.S.
Hyperlipidemia	+/-	4 / 9	8 / 47	6 / 15	N.S.

N.S.: Not significant; [a]: NBNC *vs.* B and C; [b]: NBNC *vs.* C

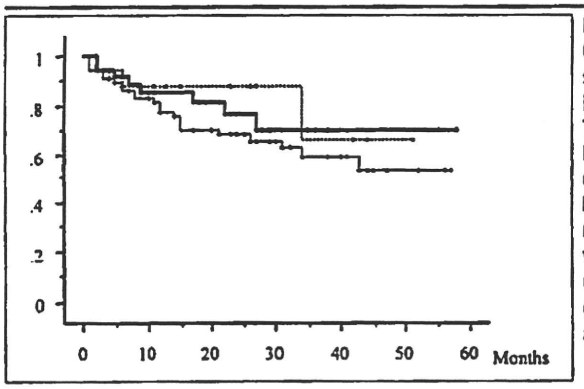

FIGURE 1
Cumulative overall survival curves for HCC after surgery. The bold line, dotted line, and thin line denote groups NBNC, B, and C, respectively. There were no significant differences in the overall survival rates among the 3 groups.

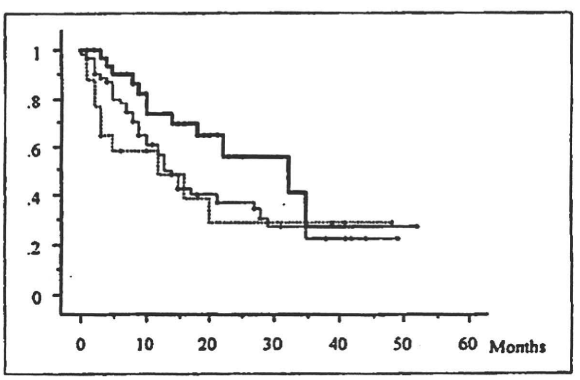

FIGURE 2
Disease-free survival curves for HCC after surgery. The bold line, dotted line, and thin line denote groups NBNC, B, and C, respectively. There were no significant differences in the disease-free survival rates among the 3 groups.

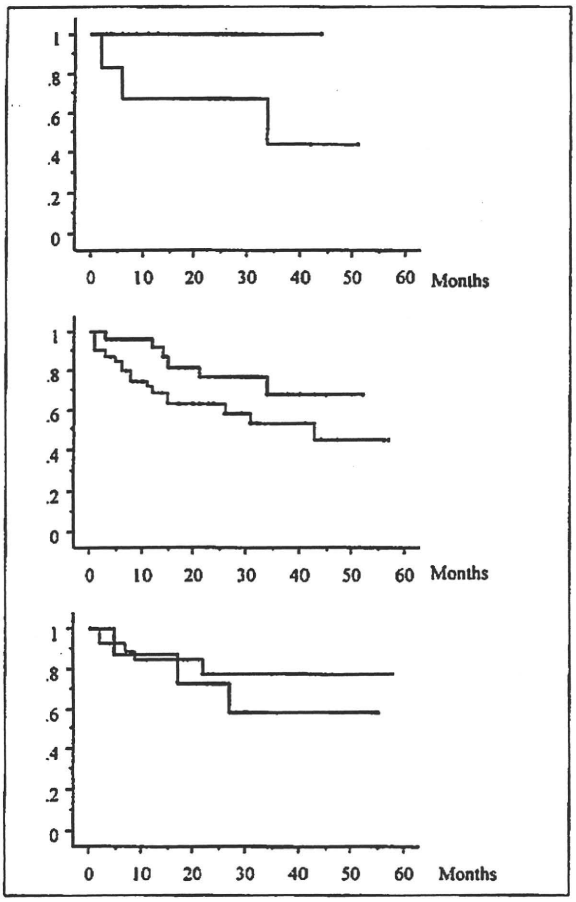

FIGURE 3
Cumulative overall survival curves with or without risk factors of metabolic syndrome.Upper panel: group B; middle panel: group C; and lower panel: group NBNC. The thin and bold lines denote patients with and without risk factors of metabolic syndrome, respectively. There were no significant differences among all groups, although groups B and C with risk factors for metabolic syndrome had a tendency toward lower survival rates than those without.

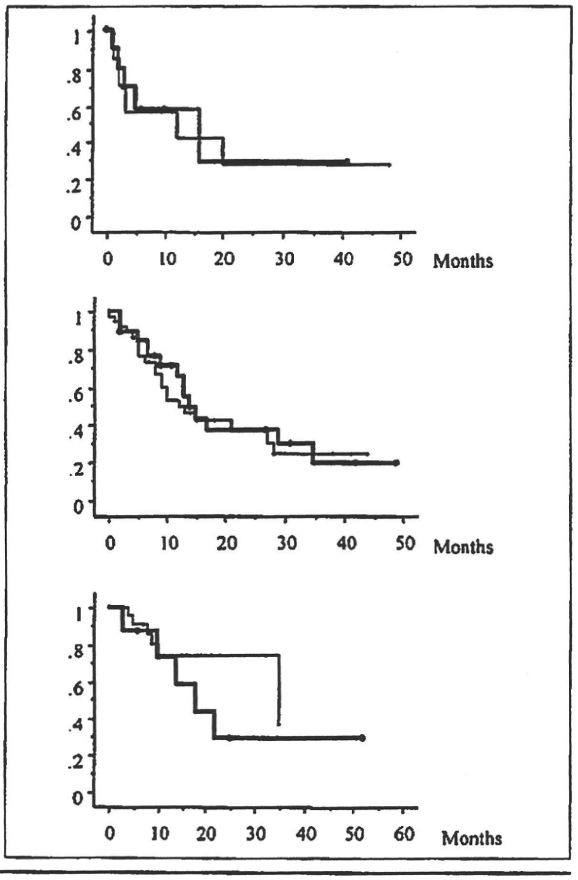

FIGURE 4
Disease-free survival curves with or without risk factors of metabolic syndrome.Upper panel: group B; middle panel: group C; and lower panel: group NBNC. The thin and bold lines denote patients with and without risk factors of metabolic syndrome, respectively. There were no significant differences among all groups.

with or without HBcAb (data not shown).

Seven out of the 37 patients from the NBNC group showed various degrees of fatty changes in their liver histology. Among them, 3 patients who did not have a history of alcohol abuse were strongly suspected to have NASH (8.1%). The clinical features of these 3 patients with HCC associated with NASH are shown in **Table 5**. We estimated both the necroinflammatory grade and the fibrosis score according to the definitions proposed by Brunt *et al.* (27). The BMIs of these three patients were 23.1, 24.8, and 24.4, respectively. These figures were within the normal range according to western standards but are considered to be overweight by Asian standards (28). Two of the 3 patients had associated diabetes mellitus, and 1 patient had no risk factors for MS.

DISCUSSION

In this study, the background and associated conditions of patients with HCC who underwent surgery in relation to viral markers was investigated, and then compared to determine participation of risk factors for MS in the development of HCC, in particular non-B non-C HCC. At first, the prevalence of chronic hepatitis and liver cirrhosis in non-B non-C HCC was confirmed to be almost the same as in group B, and was significantly lower than in group C, although there were no differences in the preoperative Child-Pugh classifications among the 3 groups.

One of the current topics in this field is the relationship between obesity and HCC (15,18). In this study, the mean BMI was less than 25kg/m^2 in all 3 groups, and there were no significant differences among them. However, the NBNC group showed the highest ratio of patients with a BMI greater than 25kg/m^2, suggesting the possible participation of obesity in non-B non-C HCC.

This study also demonstrated that patients in NBNC group had a significantly higher prevalence of both diabetes mellitus and hyperlipidemia, and their mean serum TG was significantly higher than groups B and C. This result showed that non-B non-C HCC may be strongly associated with metabolic or insulin resistance syndrome, as suggested in other reports (16,20). Diabetes mellitus has been recognized as a risk factor of not only chronic liver disease, but also HCC (14-17). Bugianesi *et al.* (20) reported that the prevalence of diabetes and the plasma levels of both TC and TG were significantly higher in those patients with HCC associated with cryptogenic cirrhosis than in patients with alcohol and hepatitis virus infection related HCC. However, in this study, the prevalence of alcohol abuse was significantly higher in the NBNC group than in group C. Therefore, we performed an additional analysis after excluding those patients with alcohol abuse. Based on that analysis, no significant difference in the prevalence of diabetes mellitus and hyperlipidemia among the 3 groups was found, although the serum TG and TC levels were still higher. In contrast to these results, some studies have indicated that alco-

Table 5 Three cases of HCC associated with NASH

	Case 1	Case 2	Case 3
Age	69	72	79
Gender	Male	Female	Male
BMI (kg/m^2)	23.1	24.8	24.4
Diabetes mellitus	-	+	+
Hypertension	-	+	-
Hyperlipidemia	-	+	+
AST (IU/L)	23	59	59
ALT (IU/L)	23	46	76
PLT (×10^4/mm^3)	15.6	16	11.8
Total Cholesterol (mg/dL)	212	217	207
Triglyceride (mg/dL)	70	95	205
Steatosis*	mild	moderate	moderate
Degeneration of hepatocyte*	mild	ballooning and acidophilic bodies	Mallory bodies and acidophilic bodies
Intraacinar inflammatory cells*	scattered microabscess	many microabscess	many microabscess
Portal inflammation*	mild	moderate to severe	moderate to severe
Necroinflammatory grade*	1	2	3
Fibrosis stage*	3	4	4

*Definitions according to Brunt *et al.* (27)

hol intake was associated with a lower prevalence of MS (29,30). In the patients studied here, however, chronic liver disease, risk factors for MS, and alcohol abuse might all participate in the carcinogenesis of HCC in a very complex fashion.

More recently, NAFLD including NASH has been considered to be one of the causes of chronic liver disease (15,31) and HCC (19-25). Although the prevalence of NASH in HCC patients remains unknown, in the literature, HCC has been observed in 2.4-13% of NASH patients (21,23,24). Bugianesi *et al.* (20) reported that among 641 cirrhosis-associated HCCs, 44 patients (6.9%) had cryptogenic cirrhosis which was associated with NASH. On the other hand, Yano *et al.* (12) stated that there were no non-B non-C patients with HCC in whom NASH was thought to be the cause. However, it is difficult to clearly determine the participation of NASH in the pathogenesis of HCC associated with cryptogenic cirrhosis, because the steatosis might decrease or disappear when the NASH progressed to cirrhosis (17,18,20,23,31). In the present study, 3 patients were judged to be associated with NASH based on microscopic findings of moderate to severe macrovesicular steatosis, hepatocellular ballooning, lobular inflammation with necrosis of the hepatocytes, and perisinusoidal fibrosis. Although there was some discussion about the histopathological findings in NAFLD (19), macro-vesicular steatosis, Mallory's hyaline, ballooning, lobular inflammation, and perisinusoidal fibrosis were considered to be histological features in general (19,31,32).

In this study, the cumulative overall and disease free 3-year survival rates for HCC in the non-B non-C patients after surgery were 69.8% and 27.6%, respectively, and there were no significant differences in both the cumulative overall and disease free survival rates among the B, C, and NBNC patients. Although this study population contained 26 patients who had already underwent some treatment for HCC, these results were considered to be almost the same as with previous studies (8,10,11,33). HCC in the non-B non-C patients has been reported to have a worse prognosis than HCC due to other causes. With respect to the influence of the risk factors for MS on survival, the interesting result was obtained that these risk factors might exhibit an adverse effect on the survival of hepatitis virus related HCC patients, but not on non-B non-C HCC patients, although their survival rates did not show any statistically significant differences because of the small number of cases studied. One could speculate that the risk factors for MS had a positive impact on the occurrence of non-B non-C HCC, but may exert a negative impact on the prognosis of hepatitis virus related HCC patients.

In conclusion, the prevalence of diabetes mellitus, hyperlipidemia, and the plasma triglyceride level were all significantly higher in non-B non-C HCC patients as compared with those with HCC related to both HBV and HCV infection. This suggests that the pathogenesis of non-B non-C HCC was more closely associated with the risk factors for MS than viral related HCC. However, alcohol abuse affected the pathological mechanisms at least in part. With respect to the participation of NASH, 3 out of 37 non-B non-C HCC patients were clearly associated with NASH from the viewpoint of their clinical and histological analyses. The prognosis of patients with positive viral markers tended to be worse in those patients who also had risk factors for MS than those without. On the other hand, there was no such tendency in the non-B non-C patients. To our knowledge, this is the first report of its kind on HCC patients with and without hepatitis virus markers, and the findings presented here may be informative in a clinical setting.

REFERENCES

1 Llovet JM, Burroughs A, Bruix J: Hepatocellular carcinoma. Lancet 2003; 362:1907-1917.
2 Ercolani G, Grazi GL, Ravaioli M, Del Gaudio M, Gardini A, Cescon M, Varotti G, Cetta F, Cavallari A: Liver resection for hepatocellular carcinoma on cirrhosis: univariate and multivariate analysis of risk factors for intrahepatic recurrence. Ann Surg 2003; 237:536-543.
3 Fong Y, Sun RL, Jarnagin W, Blumgart LH: An analysis of 412 cases of hepatocellular carcinoma at a Western center. Ann Surg 1999; 229:790-800.
4 Kiyosawa K, Sodeyama T, Tanaka E, Gibo Y, Yoshizawa K, Nakano Y, Furuta S, Akahane Y, Nishioka K, Purcell RH, Alter HJ: Interrelationship of blood transfusion, non-A, non-B hepatitis and hepatocellular carcinoma: analysis by detection of antibody to hepatitis C virus. Hepatology 1990; 12:671-675.
5 Nishioka K, Watanabe J, Furuta S, Tanaka E, Iino S, Suzuki H, Tsuji T, Yano M, Kuo G, Choo QL, Houghton M, Oda T: A high prevalence of antibody to the hepatitis C virus in patients with hepatocellular carcinoma in Japan. Cancer 1991; 67:429-433.
6 Takenaka K, Yamamoto K, Taketomi A, Itasaka H, Adachi E, Shirabe K, Nishizaki T, Yanaga K, Sugimachi K: A comparison of the surgical results in patients with hepatitis B *versus* hepatitis C-related hepatocellular carcinoma. Hepatology 1995; 22:20-24.
7 Kato Y, Nakata K, Omagari K, Furukawa R, Kusumoto Y, Mori I, Tajima H, Tanioka H, Yano M, Nagataki S: Risk of hepatocellular carcinoma in patients with cirrhosis in Japan. Analysis of infectious hepatitis viruses. Cancer 1994; 74:2234-2238.
8 Koike Y, Shiratori Y, Sato S, Obi S, Teratani T, Imamura M, Hamamura K, Imai Y, Yoshida H, Shiina S, Omata M: Risk factors for recurring hepatocellular carcinoma differ according to infected hepatitis virus-an analysis of 236 consecutive patients with a single lesion. Hepatology 2000; 32:1216-1223.
9 Shim J, Kim BH, Kim NH, Dong SH, Kim HJ, Chang YW, Lee JI, Chang R: Clinical features of HBsAg-negative but anti-HBc-positive hepatocellular carcinoma in a hepatitis B virus endemic area. J Gastroenterol Hepatol 2005; 20:746-751.
10 Uchiyama K, Ueno M, Hama T, Kawai M, Tani M, Terasawa H, Ozawa S, Uemura R, Nakase T, Yamaue H: Recurrence of primary hepatocellular carcinoma after hepatectomy--differences related to underlying hepatitis virus species. Hepatogastroenterology 2005; 52:591-595.
11 Yamanaka N, Tanaka T, Tanaka W, Yamanaka J, Yasui C, Kuroda N, Takada M, Okamoto E: Correlation of hepatitis virus serologic status with clinicopathologic features in patients undergoing hepatectomy for hepatocellular carcinoma. Cancer 1997; 79:1509-1515.
12 Yano Y, Yamashita F, Sumie S, Ando E, Fukumori K, Kiyama M, Oyama T, Kuroki S, Kato O, Yamamoto H, Tanaka M, Sata M: Clinical features of hepatocellular carcinoma seronegative for both HBsAg and anti-HCV antibody but positive for anti-HBc antibody in Japan. Am J Gastroenterol 2002; 97:156-161.
13 Expert Panel on Detection, Evaluation, and Treatment of High Blood Cholesterol in Adults: Executive summary of the third report of the national cholesterol education program (ncep) expert panel on detection, evaluation, and treatment of high blood cholesterol in adults (adult treatment panel iii). Jama 2001; 285:2486-2497.
14 Adami HO, Chow WH, Nyren O, Berne C, Linet MS, Ekbom A, Wolk A, McLaughlin JK, Fraumeni JF Jr: Excess risk of primary liver cancer in patients with diabetes mellitus. J Natl Cancer Inst 1996; 88:1472-1477.
15 Caldwell SH, Crespo DM, Kang HS, Al-Osaimi AM: Obesity and hepatocellular carcinoma. Gastroenterology 2004; 127:S97-103.
16 Davila JA, Morgan RO, Shaib Y, McGlynn KA, El-Serag HB: Diabetes increases the risk of hepatocellular carcinoma in the United States: a population based case control study. Gut 2005; 54:533-539.
17 El-Serag HB, Tran T, Everhart JE: Diabetes increases the risk of chronic liver disease and hepatocellular carcinoma. Gastroenterology 2004; 126:460-468.
18 Powell EE, Jonsson JR, Clouston AD: Steatosis: co-factor in other liver diseases. Hepatology 2005; 42:5-13.
19 Brunt EM: Nonalcoholic steatohepatitis. Semin Liver Dis 2004; 24:3-20.
20 Bugianesi E, Leone N, Vanni E, Marchesini G, Brunello F, Carucci P, Musso A, De Paolis P, Capussotti L, Salizzoni M, Rizzetto M: Expanding the natural history of nonalcoholic steatohepatitis: from cryptogenic cirrhosis to hepatocellular carcinoma. Gastroenterology 2002; 123:134-140.
21 Marrero JA, Fontana RJ, Su GL, Conjeevaram HS, Emick DM, Lok AS: NAFLD may be a common underlying liver disease in patients with hepatocellular carcinoma in the United States. Hepatology 2002; 36:1349-1354.
22 Mori S, Yamasaki T, Sakaida I, Takami T, Sakaguchi E, Kimura T, Kurokawa F, Maeyama S, Okita K: Hepatocellular carcinoma with nonalcoholic steatohepatitis. J Gastroenterol 2004; 39:391-396.
23 Powell EE, Cooksley WG, Hanson R, Searle J, Halliday JW, Powell LW: The natural history of nonalcoholic steatohepatitis: a follow-up study of forty-two patients for up to 21 years. Hepatology 1990; 11:74-80.
24 Shimada M, Hashimoto E, Taniai M, Hasegawa K, Okuda H, Hayashi N, Takasaki K, Ludwig J: Hepatocellular carcinoma in patients with non-alcoholic steatohepatitis. J Hepatol 2002; 37:154-160.
25 Zen Y, Katayanagi K, Tsuneyama K, Harada K, Araki I, Nakanuma Y: Hepatocellular carcinoma arising in nonalcoholic steatohepatitis. Pathol Int 2001; 51:127-131.
26 Liver Cancer Study Group of Japan (Eds.): The General Rules for the Clinical and Pathological Study of Primary Liver Cancer. 4th Edition. Tokyo: Kanehara, 2000.
27 Brunt EM, Janney CG, Di Bisceglie AM, Neuschwander-Tetri BA, Bacon BR: Nonalcoholic steatohepatitis: a proposal for grading and staging the histological lesions. Am J Gastroenterol 1999; 94:2467-2474.
28 Weisell RC: Body mass index as an indicator of obesity. Asia Pac J Clin Nutr 2002; 11:S681-684.
29 Freiberg MS, Cabral HJ, Heeren TC, Vasan RS, Curtis Ellison R: Alcohol consumption and the prevalence of the Metabolic Syndrome in the US: a cross-sectional analysis of data from the Third National Health and Nutrition Examination Survey. Diabetes Care 2004; 27:2954-2959.
30 Djousse L, Arnett DK, Eckfeldt JH, Province MA, Singer MR, Ellison RC: Alcohol consumption and metabolic syndrome: does the type of beverage matter? Obes Res 2004; 12:1375-1385.
31 Sanyal AJ: AGA technical review on nonalcoholic fatty liver disease. Gastroenterology 2002; 123:1705-1725.
32 Angulo P: Nonalcoholic fatty liver disease. N Engl J Med 2002; 346:1221-1231.
33 Lang H, Sotiropoulos GC, Domland M, Fruhauf NR, Paul A, Husing J, Malago M, Broelsch CE: Liver resection for hepatocellular carcinoma in non-cirrhotic liver without underlying viral hepatitis. Br J Surg 2005; 92:198-202.

Diabetic KK-A^{y} mice are highly susceptible to oxidative hepatocellular damage induced by acetaminophen

Kazuyoshi Kon, Kenichi Ikejima, Kyoko Okumura, Kumiko Arai, Tomonori Aoyama and Sumio Watanabe

Am J Physiol Gastrointest Liver Physiol 299:G329-G337, 2010. First published 10 June 2010; doi:10.1152/ajpgi.00361.2009

Am J Physiol Gastrointest Liver Physiol 299: G329–G337, 2010.
First published June 10, 2010; doi:10.1152/ajpgi.00361.2009.

Diabetic KK-A^y mice are highly susceptible to oxidative hepatocellular damage induced by acetaminophen

Kazuyoshi Kon,[1] Kenichi Ikejima,[1,2] Kyoko Okumura,[1] Kumiko Arai,[1] Tomonori Aoyama,[1,2] and Sumio Watanabe[1,2]

[1]*Department of Gastroenterology, Juntendo University School of Medicine, and* [2]*Sportology Center, Juntendo University Graduate School of Medicine, Tokyo, Japan*

Submitted 4 September 2009; accepted in final form 3 June 2010

Kon K, Ikejima K, Okumura K, Arai K, Aoyama T, Watanabe S. Diabetic KK-A^y mice are highly susceptible to oxidative hepatocellular damage induced by acetaminophen. *Am J Physiol Gastrointest Liver Physiol* 299: G329–G337, 2010. First published June 10, 2010; doi:10.1152/ajpgi.00361.2009.—Despite pathophysiological similarities to alcoholic liver disease, susceptibility to acetaminophen hepatotoxicity in metabolic syndrome-related nonalcoholic steatohepatitis (NASH) has not been well elucidated. In this study, therefore, we investigated acetaminophen-induced liver injury in KK-A^y mice, an animal model of metabolic syndrome. Twelve-week-old male KK-A^y and C57Bl/6 mice were injected intraperitoneally with 300 or 600 mg/kg acetaminophen, and euthanized 6 h later. Liver histology was assessed, and hepatic expression of 4-hydroxy-2-nonenal was detected by immunohistochemistry. Levels of reduced glutathione were determined spectrophotometrically. Phosphorylation of c-Jun NH_2-terminal kinase (JNK) was analyzed by Western blotting. Hepatocytes were isolated from both strains by collagenase perfusion, and cell death and oxidative stress were measured fluorometrically by use of propidium iodide and 5-(and-6)-chloromethyl-2′7′-dichlorodihydrofluorescein diacetate acetyl ester, respectively. Acetaminophen induced more severe necrosis and apoptosis of hepatocytes in KK-A^y mice than in C57Bl/6 mice and significantly increased serum alanine aminotransferase levels in KK-A^y mice. Acetaminophen-induction of 4-hydroxy-2-nonenal in the liver was potentiated, whereas the levels of reduced glutathione in liver were lower in KK-A^y mice. Acetaminophen-induced phosphorylation of JNK in the liver was also enhanced in KK-A^y mice. Exposure to 20 μM *tert*-butyl hydroperoxide did not kill hepatocytes isolated from C57Bl/6 mice but induced cell death and higher oxidative stress in hepatocytes from KK-A^y mice. These results demonstrated that acetaminophen toxicity is increased in diabetic KK-A^y mice mainly due to enhanced oxidative stress in hepatocytes, suggesting that metabolic syndrome-related steatohepatitis is an exacerbating factor for acetaminophen-induced liver injury.

drug-induced liver injury; metabolic syndrome; steatohepatitis; oxidative stress; hepatotoxicity

ACETAMINOPHEN OVERDOSE IS the leading cause of acute liver failure in the United States (22). Acetaminophen toxicity accounts for ~50% of all cases of acute liver failure in the United States and carries a 30% mortality (35). In the development of acetaminophen hepatotoxicity, overdosed acetaminophen is metabolized by cytochrome P450 (CYP) 2E1 (25) and forms a chemically reactive metabolite, *N*-acetyl-*p*-benzoquinonimine (NAPQI). NAPQI reacts with glutathione (GSH) (20) thereby forming an acetaminophen-GSH conjugate (6) and GSH depletion (29). Acetaminophen has long been recognized as a dose-dependent toxin, and most cases of acetaminophen-induced liver failure are suicidal overdose more than 15 g; however, in some cases, people develop acute liver failure although they do not take doses of acetaminophen exceeding the amount recommended on the package labeling of up to 4 g daily (22). Since unintentional acetaminophen-induced liver injury tends to be treated late with antidote *N*-acetylcysteine, it is extremely important to investigate the risk factor for increasing susceptibility to acetaminophen-induced liver injury.

Nonalcoholic steatohepatitis (NASH) is the syndrome diagnosed following liver biopsy results that are consistent with alcoholic hepatitis and/or fibrosis although patients deny significant alcohol use. NASH has been consistently associated with metabolic syndrome including obesity, diabetes mellitus, hypertension, dyslipidemia, and insulin resistance (18, 26, 38, 42), and it has been proposed that simple steatosis can progress to NASH (7). Recently, it was reported that nonalcoholic fatty liver disease (NAFLD) conveys a nearly fourfold increase of risk for liver injury caused by various drugs. Some exacerbating drug treatments include antihypertensive medication, drugs that inhibit platelet aggregation, antimicrobials, nonsteroidal anti-inflammatories, and proton pump inhibitors prescribed to obese middle-aged patients (41). Although it is well known that alcohol use is an important risk factor of acetaminophen-induced liver injury (33, 43), the impact of NAFLD on acetaminophen hepatotoxicity still remains unclear.

KK-A^y mice are a strain derived from crossing the diabetic KK mouse (13) with the lethal yellow (A^y) mouse, which carry a mutation of the agouti (a) gene in chromosome 2 (28, 40). KK-A^y mice exhibit phenotypes including obesity, dyslipidemia, and insulin resistance, which resemble metabolic syndrome in human (1, 11, 15). We have reported that KK-A^y mice develop steatohepatitis spontaneously and exhibit increased susceptibility to methionine- and choline-deficiency diet-induced steatohepatitis (32). In the present study, we investigated the sensitivity of KK-A^y mice to acetaminophen hepatotoxicity to address the influence of steatosis and steatohepatitis on acetaminophen-induced liver injury.

MATERIALS AND METHODS

Animals and experimental design. Male KK-A^y and C57Bl/6 mice were purchased from CLEA Japan (Tokyo, Japan). Mice were housed in air-conditioned, specific pathogen-free animal quarters with lighting from 0800 to 2100 and were given unrestricted access to a standard laboratory chow and water throughout this study. All animals received humane care, and the experimental protocol was approved by the Committee of Laboratory Animals according to institutional guidelines. C57Bl/6 mice, which are the strains of two generations ago, were selected as nonobese and nondiabetic controls. After acclimation, both KK-A^y and C57Bl/6 mice at 12 wk of age were separated into three groups randomly, and some mice were injected with 300 or

Address for reprint requests and other correspondence: K. Ikejima, 2-1-1 Hongo, Bunkyo-ku, Tokyo, 113-8421 Japan (e-mail: ikejima@juntendo.ac.jp).

600 mg/kg acetaminophen intraperitoneally. Control groups were injected with physiological saline solution alone. After administration of acetaminophen for 6 h, mice were killed by exsanguination by snipping the inferior vena cava, followed by collection of liver and serum samples.

Histological analysis. For histological evaluations, liver tissues were fixed in 10% buffered formalin and embedded in paraffin, and hematoxylin-eosin staining was performed. To detect apoptotic cell death in tissue, the terminal deoxynucleotidyl transferase-mediated dUTP nick-end labeling (TUNEL) assay was performed by using a commercial kit according to the manufacturer's instructions (In Situ Cell Death Detection Kit, Fluorescein, Roche, Indianapolis, IN). TUNEL-positive staining was assessed by using a green nuclear fluorescence dye and was compared with a total nuclei stain, propidium iodide (PI). Staining was quantified by use of laser scanning confocal microscopy (Zeiss 410; Carl Zeiss, Thornwood, NY) and was performed on more than 500 hepatocytes per animal. TUNEL staining was expressed as the number of positively stained nuclei divided by the total number of nuclei.

Immunohistochemistry. The expression and localization of tissue 4-hydroxy-2-nonenal (4-HNE) in the liver was detected by immunohistochemical staining as previously described elsewhere (32). Briefly, deparaffinized tissue sections were incubated with a monoclonal anti-4-HNE antibody (Japan Institute for the Control of Aging, Nikken SEIL, Shizuoka, Japan) and a secondary biotinylated anti-mouse IgG. The specific binding was visualized with the avidin-biotin complex solution followed by incubation with a 3,3-diaminobenzidine tetrahydrochloride solution by use of Vectastain Elite ABC kit (Vector Laboratories, Burlingame, CA). Specimens for histology and immunohistochemistry were observed under an optical microscope (PH-2; Olympus, Tokyo, Japan) equipped with a digital microscope camera (VB6000; Keyence, Osaka, Japan).

Measurement of serum aminotransferase levels. Serum alanine aminotransferase (ALT) levels were measured spectrophotometrically

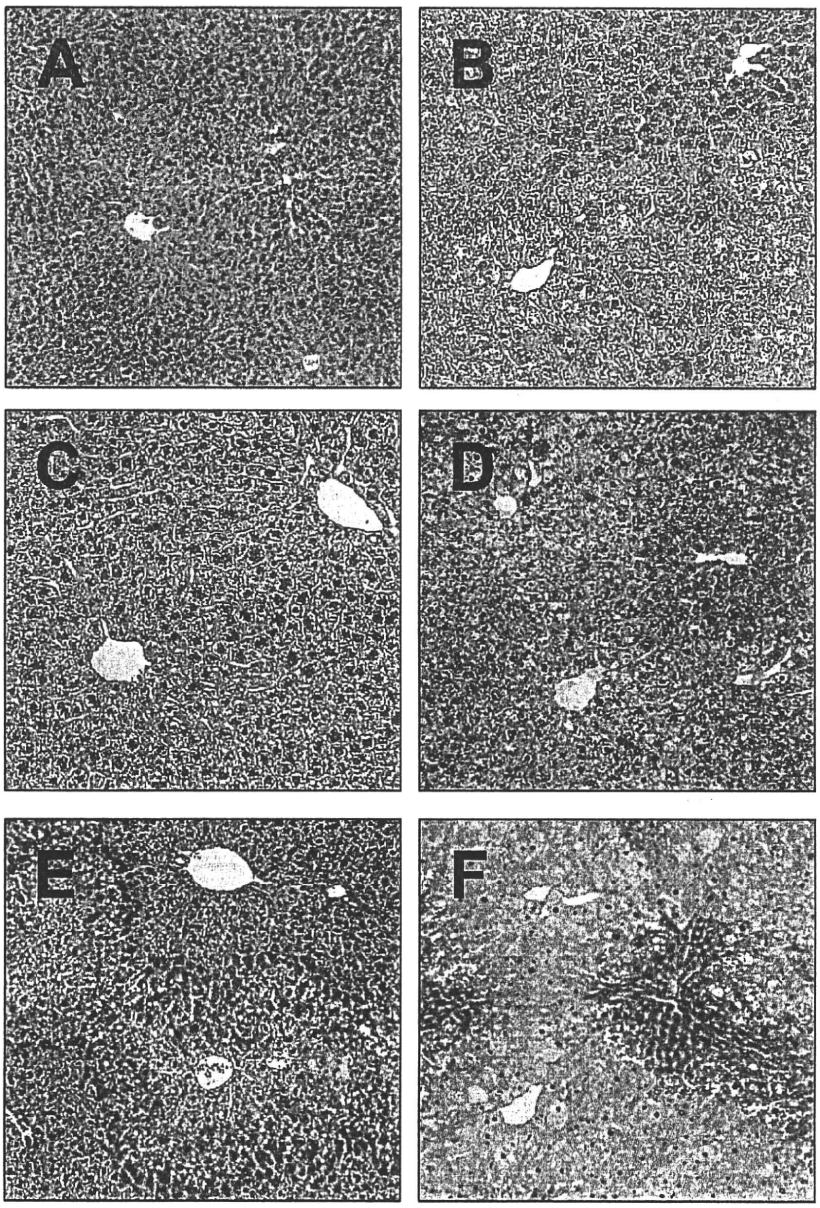

Fig. 1. Effect of acetaminophen on liver histology in KK-A^y mice. C57Bl/6 and KK-A^y mice were given a single intraperitoneal injection of acetaminophen (300–600 mg/kg body wt), and euthanized 6 h later. Representative photomicrographs (n = 5) of the liver from C57Bl/6 saline controls (*A*), KK-A^y mice saline controls (*B*), C57Bl/6 mice treated with 300 mg/kg acetaminophen (*C*), KK-A^y mice treated with 300 mg/kg acetaminophen (*D*), C57Bl/6 mice treated with 600 mg/kg acetaminophen (*E*), KK-A^y mice treated with 600 mg/kg acetaminophen (*F*), are shown with hematoxylin-eosin staining at an original magnification of ×100.

by a standard enzymatic method using a commercial kit (KAINOS Laboratories, Tokyo, Japan).

Lipid peroxidation assay and measurement of GSH in the liver. The tissue contents of malondialdehyde (MDA)/4-hydroxyalkenals (HAE) were measured colorimetrically using the lipid peroxidation assay kit (Calbiochem, EMD Biosciences, San Diego, CA). Briefly, the whole liver was homogenized in ice-cold phosphate-buffered saline (PBS) containing 5 mM butylated hydroxytoluene and was centrifuged at 3,000 *g* for 10 min to collect the supernatant. Samples were then incubated with *N*-methyl-2-phenylindole in methanol:acetonitrile and methanesulfonic acid at 45°C for 60 min, and the absorbance at 586 nm was measured spectrophotometrically. Reduced GSH levels in the liver tissue samples were measured using a commercial kit (OXIS International, Portland, OR) according to the manufacturer's instructions.

Western blot analysis. Protein extracts were obtained by homogenizing frozen tissues in a buffer containing 50 mM Tris, pH 8.0, 150 mM NaCl, 1 mM ethylenediaminetetraacetic acid, 1% Triton X-100, and protease inhibitors (Complete Mini, Roche Diagnostics, Mannheim, Germany) followed by centrifugation at 17,400 *g* for 15 min, and the protein concentration was determined by use of a Bio-Rad protein assay kit (Bio-Rad Laboratories, Hercules, CA). Five micrograms of protein was separated in 12.5% sodium dodecyl sulfate (SDS)-polyacrylamide gel electrophoresis and electrophoretically transferred onto polyvinylidene fluoride membranes. After blocking with 5% nonfat dry milk in Tris-buffered saline, membranes were incubated with a primary rabbit polyclonal anti-phospho-stress-activated protein kinase (SAPK)/c-Jun NH_2-terminal kinase (JNK) (Thr183/Tyr185) antibody (Cell Signaling Technology, Danvers, MA), followed by a secondary horseradish peroxidase (HRP)-conjugated anti-rabbit IgG antibody (DakoCytomation Norden). Subsequently, specific bands were visualized using the ECL detection kit (Amersham Pharmacia Biotech, Piscataway, NJ). The membranes were stripped by incubation in a buffer containing 100 mM 2-mercaptoethanol, 2% SDS, and 62.5 mM Tris·HCl, pH 6.7, at 50°C for 30 min and reprobed with rabbit anti-SAPK/JNK polyclonal antibody (Cell Signaling Technology) and secondary HRP-conjugated anti-rabbit IgG antibody.

Isolation and primary culture of mouse hepatocytes. Hepatocytes were isolated from both strains by in situ collagenase perfusion and differential centrifugations as previously described (21). Hepatocytes were resuspended in Waymouth's medium MB-752/1 containing 2 mM L-glutamine, 10% fetal bovine serum, 100 nM insulin, 100 nM dexamethasone, 100 units/ml penicillin, and 100 μg/ml streptomycin. Cell viability was greater than 90%, as determined by Trypan blue exclusion. Hepatocytes were plated in a 24-well microtiter plates (1.5×10^5 cells per well) or 35-mm Petri dishes (6×10^5 cells per dish, Falcon, Lincoln Park, NJ). Plates and coverslips were coated with 0.1% Type 1 rat-tail collagen. Hepatocytes were preincubated in humidified 5% CO_2-95% air at 37°C, and medium was replaced with Krebs-Ringer-HEPES buffer (KRH) containing 115 mM NaCl, 5 mM KCl, 2 mM $CaCl_2$, 1 mM KH_2PO_4, 1.2 mM $MgSO_4$, and 25 mM HEPES (pH 7.4) at 37°C after overnight incubation (19).

Fluorometric assay of cell viability and oxidative stress in primary cultured hepatocytes. Cell death and production of oxidative stress in isolated hepatocytes was determined fluorometrically by using PI and 5-(and-6)-chloromethyl-2′7′-dichloro-dihydrofluorescein diacetate acetyl ester (CMH_2DCF), respectively. After attachment to 24-well plates, hepatocytes were washed once and replaced with KRH buffer containing 30 μM PI. Fluorescence was measured by using a multiwell fluorescence reader (Fluoroskan Ascent, Thermo Fisher Scientific, Waltham, MA), as previously described elsewhere (31). Cell death assessed by PI fluorometry correlates closely with Trypan blue exclusion and enzyme release as indicators of oncotic necrosis.

Oil red O staining. Triglycerides in hepatocytes were visualized by Oil Red O staining. Overnight cultured hepatocytes were fixed

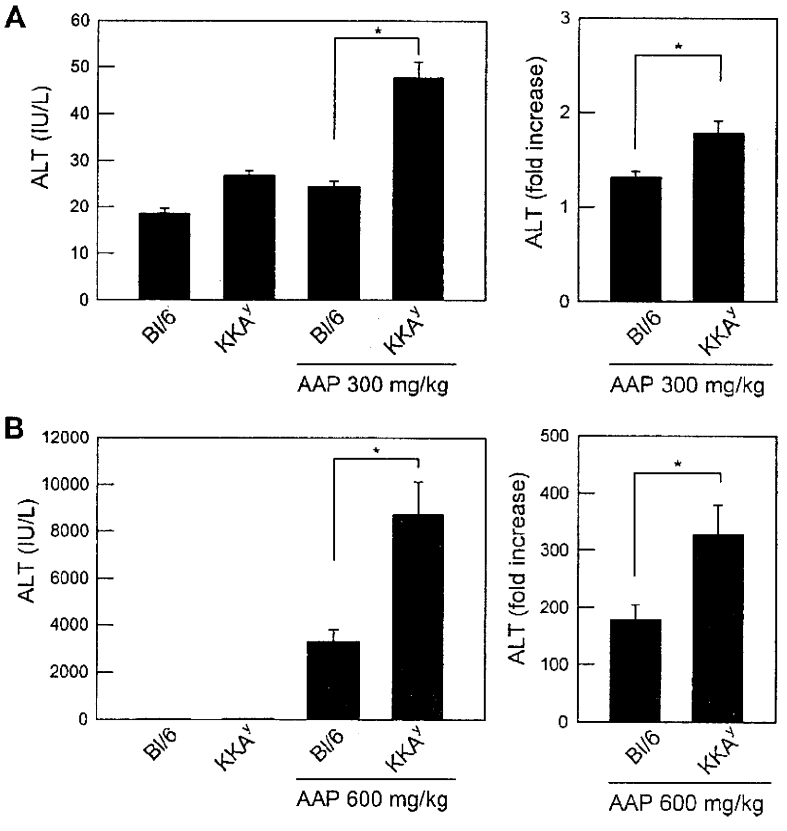

Fig. 2. Effect of acetaminophen on serum alanine aminotransferase (ALT) levels in KK-A^{Y} mice. Mice were treated with 300 mg/kg (*A*) or 600 mg/kg (*B*) acetaminophen (AAP), and serum samples were collected 6 h later. Serum ALT levels were measured by the colorimetric method, and average values (*left*) and the ratio vs. control values in each strain (*right*) are plotted; $n = 5$, $^{*}P < 0.05$ vs. C57Bl/6+acetaminophen, by ANOVA on ranks and Student-Newman-Keuls post hoc test.

with 4% formaldehyde for 10 min and then stained with Oil Red O for 1 h followed by washing with 60% methanol and PBS. Cells were photographed by using a phase-contrast microscope equipped with a digital sight camera system (DS-5M-L1, Nikon, Japan).

Statistical analysis. Morphometrical and densitometric analyses were performed with Scion Image (version Beta 4.0.2, Scion, Fredrick, MD). Data were expressed as means ± SE. Statistical differences between means were determined by Student's *t*-test, one-way analysis of variance (ANOVA), or Kruskal-Wallis ANOVA on ranks followed by an all-pairwise multiple-comparison procedure (Student-Newman-Keuls method) as appropriate. $P < 0.05$ was selected before the study to reflect significance.

RESULTS

Acetaminophen causes severe liver injury in KK-A^y mice. At first, we evaluated the sensitivity to acetaminophen-induced hepatotoxicity in KK-A^y mice by injecting two different doses (300 or 600 mg/kg) of this drug intraperitoneally. Mild liver steatosis was observed in 12-wk-old KK-A^y mice without administration of acetaminophen as expected (Fig. 1*B*). A single injection of the lower dose of acetaminophen (300 mg/kg), which did not affect liver histology in C57Bl/6 mice (Fig. 1*C*), caused mild necrotic liver injury with infiltration of inflammatory cells predominantly in pericentral area at 6 h

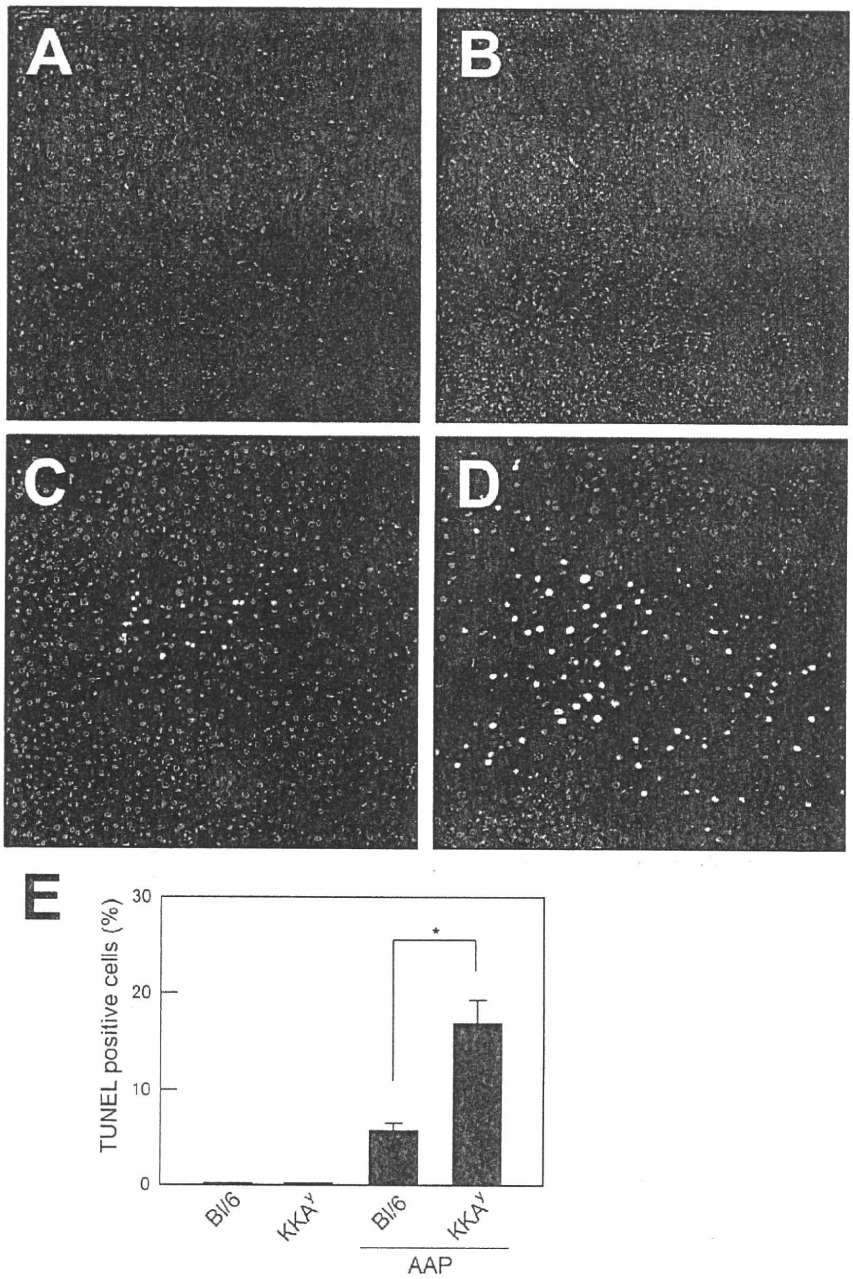

Fig. 3. Effect of acetaminophen on apoptotic cells death in the liver in KK-A^y mice. Apoptotic cells in the liver 6 h after a single injection of 600 mg/kg acetaminophen were detected by terminal deoxynucleotidyl transferase-mediated dUTP nick-end labeling (TUNEL) staining. Representative photomicrographs of the liver from C57Bl/6 mice saline controls (*A*), KK-A^y mice saline controls (*B*), C57Bl/6 mice treated with acetaminophen (*C*), and KK-A^y mice treated with acetaminophen (*D*) are shown (original magnification ×100). Number of TUNEL-positive hepatocytes was counted, and average percentages of TUNEL-positive cells from 5 different animals are plotted. More than 500 cells per 1 animal were counted (*E*). *P <0.05 vs. C57Bl/6+acetaminophen by ANOVA on ranks and Student-Newman-Keuls post hoc test.

(Fig. 1*D*). A higher dose of acetaminophen (600 mg/kg), which induced mild liver injury even in C57Bl/6 mice (Fig. 1*E*), caused extremely severe necrosis in the liver in KK-A^y mice (Fig. 1*F*).

Serum ALT levels were not changed in C57Bl/6 mice 6 h after treatment with 300 mg/kg acetaminophen (24 ± 1 IU/l) and increased significantly to 47 ± 4 IU/l in KK-A^y mice (Fig. 2*A*, *left*, $P < 0.05$). A higher dose of acetaminophen (600 mg/kg) elevated serum ALT levels to 3,281 ± 513 IU/l in C57Bl/6 mice, whereas the levels were increased significantly to 8,707 ± 1,400 IU/l in KK-A^y mice (Fig. 2*B*, *left*, $P < 0.05$) as expected. Furthermore, the ratio of acetaminophen-induced increases in ALT levels vs. control values in each strain was plotted (Fig. 2, *A* and *B*, *right*). Elevations in serum ALT levels were potentiated significantly in KK-A^y mice by both lower and higher doses of acetaminophen, indicating that KK-A^y mice are more susceptible to acetaminophen-induced liver injury.

To determine whether apoptotic cell death is involved in hepatocyte injury caused by acetaminophen, TUNEL staining was performed (Fig. 3). A few TUNEL-positive cells were observed in the liver in C57Bl/6 mice 6 h after treatment with 600 mg/kg acetaminophen (Fig. 3*C*), where the percentage of TUNEL-positive hepatocytes were 5.7 ± 0.7% (Fig. 3*E*). In KK-A^y mice after acetaminophen, the percentage of TUNEL-positive cells and necrotic cell death increased in the area

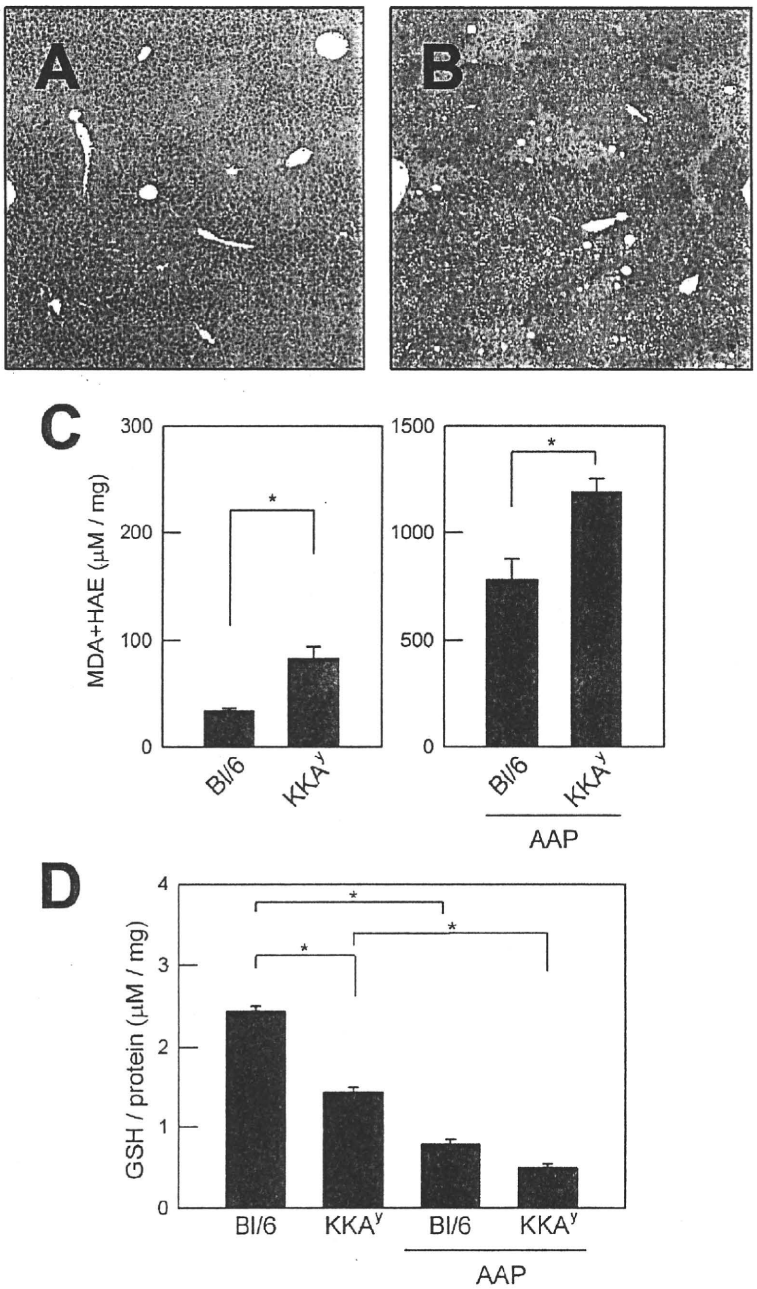

Fig. 4. Effect of acetaminophen on lipid peroxidation and glutathione content in the liver in KK-A^y mice. Hepatic expression of 4-HNE was detected by immunohistochemistry. Representative photomicrographs from C57Bl/6 mice (*A*) and KK-A^y mice (*B*) treated with 6 h after a single injection of 600 mg/kg acetaminophen are shown. Malondialdehyde (MDA)/4-hydroxyalkenals (4-HAE) levels in liver homogenates were measured colorimetrically (*C*); $n = 5$, $^*P < 0.05$ by ANOVA on ranks and Student-Newman-Keuls post hoc test. Glutathione (GSH) levels in liver homogenates were measured colorimetrically (*D*); $n = 5$, $^*P < 0.05$ by ANOVA on ranks and Student-Newman-Keuls post hoc test. Values are normalized by total protein concentrations in the homogenates.